Effect of Melt-to-Solid Insert Volume Ratio on Mg/Al Dissimilar Metals Bonding

S. M. Emami, M. Divandari, H. Arabi & E. Hajjari

Journal of Materials Engineering and Performance

ISSN 1059-9495
Volume 22
Number 1

J. of Materi Eng and Perform (2013)
22:123-130
DOI 10.1007/s11665-012-0243-y

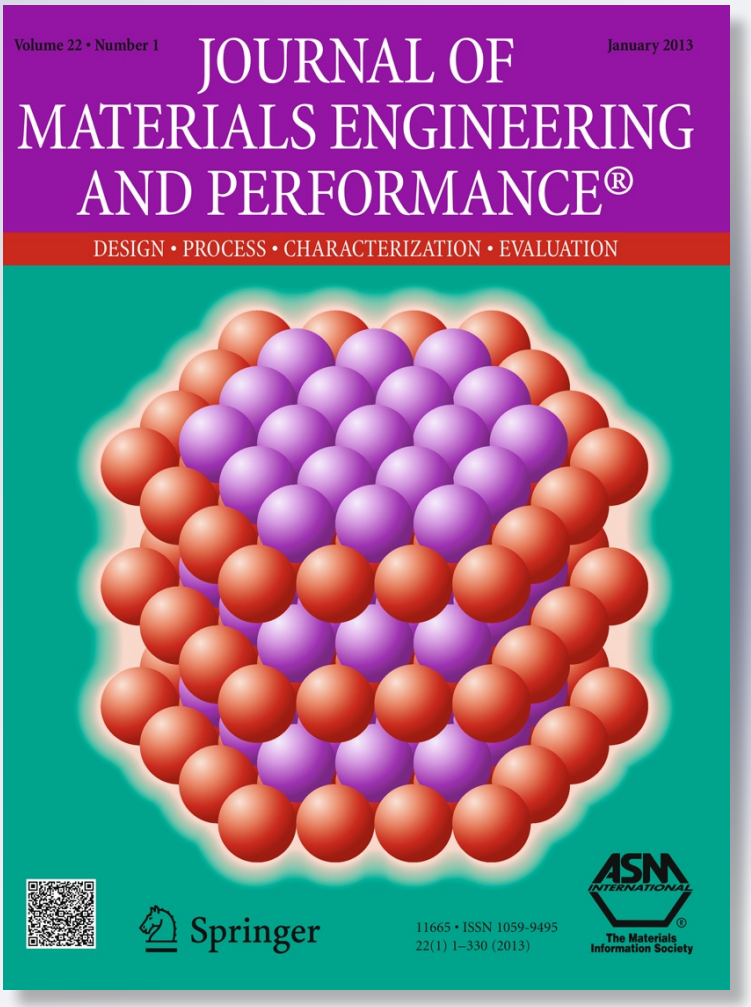

Springer

JMEPEG (2013) 22:123–130
DOI: 10.1007/s11665-012-0243-y

1059-9495/$19.00

Effect of Melt-to-Solid Insert Volume Ratio on Mg/Al Dissimilar Metals Bonding

S.M. Emami, M. Divandari, H. Arabi, and E. Hajjari

(Submitted July 10, 2011; in revised form December 22, 2011; published online May 17, 2012)

Compound casting is used as a process to join various similar and dissimilar metallic couples. The ratio of melt-to-solid volume is one of the main factors that can affect the contact time between melt and the solid insert. In this investigation, magnesium and aluminum metals (magnesium as the cast metal and aluminum as the solid insert) having melt-to-solid volume ratios (V_m/V_s) of 1.25, 3, and 5.25 were successfully bonded via compound casting. Results demonstrated that by increasing the ratio of V_m/V_s from 1.25 to 5.25, the thickness of the reaction interface between Al and Mg varies within the range of 200 to 1800 μm. X-ray diffraction, scanning electron microscopy, and Vickers microhardness study of the bonding of these two metals showed that the interface consisted of three separate sub-layers within reaction layer. These sub-layers had higher hardness than those of the Al and Mg bulk metals. In all specimens, composition of the sub-layer adjacent to Al (layer I) was Al_3Mg_2 and that adjacent to Mg (layer III) was $Al_{12}Mg_{17}$/(Mg) eutectic structure. The intermediate layer composition (layer II) in specimens with volume ratio of 1.25 and 3 was a single-phase $Al_{12}Mg_{17}$, while for the case of volume ratio 5.25 this sub-layer consisted of $Al_{12}Mg_{17}$/(Mg) eutectic dispersed in $Al_{12}Mg_{17}$ intermetallic. The results of this research showed that in low melt/solid volume ratios, diffusion-reaction was the dominant mechanism for formation of Al-Mg intermetallic. However, when V_m/V_s and the melt/solid insert contact time increased, the dominant mechanism of Al-Mg intermetallics changed to fusion-solidification due to increase in surface melting of the solid insert. Also the results of push-out tests showed that shear strengths of the interface decrease from 27.1 to 15.1 and 8.3 MPa for the Al/Mg couples prepared at 1.25, 3, and 5.25 V_m/V_s respectively.

Keywords aluminum, casting, intermetallics, joining, non ferrous metal

1. Introduction

Magnesium and aluminum with theoretical densities of 1700 and 2700 kg/m^3, respectively, are the most used engineering light metals. Magnesium alloys benefit from low density, high specific strength, and good castability, while suffer from low ductility and creep resistance. On the other hand, besides higher ductility, aluminum alloys are able to maintain their strength at higher temperatures (Ref 1, 2).Therefore, manufacturing Mg-Al compound parts seems to be a promising solution for future industrial needs and can potentially prevents many environmental problems.

Compound casting is a process of joining two metals or alloys through direct casting in which one component is in solid state and the other is in the form of melt. In this process, solid insert is mounted in the mold and commercially pure metal or alloy melt is cast around it. Hence, a diffusion reaction zone is formed at the interface of melt and solid insert that results in bonding of the two metals (Ref 3-5). Producing complicated parts, using this process is easy and less time consuming (Ref 6).

The results of several studies on various affecting parameters involved in dissimilar metals compound casting have so far been published. Among these, Noguchi et al. (Ref 7) reported that melt/solid volume ratio and casting temperature are the two important factors that affect contact time between melt and solid insert. However, a few of these researchers have used the compound casting technique to join different dissimilar and similar metallic couples such as steel/cast iron (Ref 8-10), steel/Al (Ref 11, 12), Cu/Al (Ref 13), Al/Al (Ref 5, 11, 14) and Mg/Mg (Ref 15), and Al/Mg (Ref 16). However, joining dissimilar light metals such as aluminum and magnesium by this process is still a relatively unexplored area.

It has been reported (Ref 14, 17) that a good contact with satisfactory metallurgical and mechanical properties between Mg/Al, Al/Al, and Mg/Mg couples, leads to significant increase in application of these light metals in automotive and aerospace industries. This results to a lower fuel consumption and a lower emission of greenhouse gasses.

In this research, the effect of melt-to-solid insert volume ratio (V_m/V_s) on bonding of Mg and Al through compound casting process has been investigated to establish optimized bonding between these metals.

The melt-to-solid insert volume ratios can be calculated using Eq 1

$$\frac{V_m}{V_s} = \left(\frac{r_m}{r_s}\right)^2 - 1 \qquad \text{(Eq 1)}$$

where V_m and V_s are the melt and solid insert volume, r_m and r_s are the mold and solid insert radius, respectively.

S.M. Emami, School of Metallurgy and Materials Engineering, Iran University of Science and Technology (IUST), Narmak, Tehran, Iran; **M. Divandari** and **H. Arabi**, School of Metallurgy and Materials Engineering, Center of Excellence for Advanced Materials and Processing (CEAMP), Iran University of Science and Technology (IUST), Tehran, Iran; and **E. Hajjari**, Department of Metallurgy and Materials, Faculty of Engineering, Shahid Chamran University (SCU), Ahwaz, Iran. Contact e-mail: s_emami@metaleng.iust.ac.ir.

2. Materials and Experimental Procedure

Commercially pure aluminum and magnesium were used to prepare Mg/Al couples. Chemical compositions of the materials used are given in Table 1.

To fabricate the Mg/Al couples by the compound casting process, cylindrical inserts with 20 mm diameter and 100 mm height were machined from aluminum ingots. Their surface were ground with silicon carbide papers up to 1200 grit, then rinsed with acetone and placed within a cylindrical cavity of a CO_2 sand mold with 30, 40, and 50 mm diameter and 80 mm height in three different experiments. Schematic of the mold used in the casting process is illustrated in Fig. 1.

Magnesium ingots were melted in a steel crucible placed in an electrical furnace under the Foseco MAGREX 36 covering flux, to protect magnesium melt from oxidation. The molten magnesium poured around the aluminum inserts at 700 °C under normal atmospheric condition.

After the casting process, specimens were cut from the middle part of the samples perpendicular to the cylindrical insert with the thickness of 20 mm (Fig. 2). The specimens were further ground with SiC papers (1200 grit) and polished with 1 μm diamond paste. Then, they were etched by a 1 vol.% HNO_3 in alcohol solution on the magnesium side and a 1 vol.% HF distilled in water solution on the aluminum side.

Finally, the microstructures of the specimens were examined using an Olympus BX51M optical microscope (OM) and a JEOL JSM-7000F scanning electron microscope (SEM) equipped with the energy dispersive x-ray (EDS) detector. The phase constitutions on the fracture surfaces of the specimens were also identified using a Rigaku RINT-RAPID x-ray diffractometer. A Buehler MX9660a hardness tester with a testing load of 50 g and a holding time of 20 s was used to determine the Vickers microhardness profile across the joint interface. Shear strengths of the interface were determined using push-out tests. The tests were performed using a Shimadzu AG-I 50 kN electronic universal testing machine. The specimens with a thickness of 10 mm were put on a flat supporting surface with a circular hole of 22 mm diameter and pushed by means of a steel cylinder stub punch, concentric with the support hole, with an 18 mm diameter at a cross-head displacement rate of 0.2 mm/min. At least three slices from each VR were submitted to push-out test. Shear strength of the interface (τ_{int}) was calculated using the following equation (Ref 18, 19):

$$\tau_{int} = \frac{F_{max}}{2\pi r t} \qquad \text{(Eq 2)}$$

where F_{max} is the maximum load, r is the insert radius (10 mm), and t is the specimen thickness (10 mm). Schematic of the setup used for the push-out tests is illustrated in Fig. 3.

3. Results and Discussion

OM images of Mg/Al interface are illustrated in Fig. 4. In these experiments, magnesium was cast around three 20 mm diameter cylindrical aluminum inserts, each positioned in a cylindrical mold with 30, 40, and 50 mm diameters.

It can be observed in Fig. 4, Al and Mg in all specimens reacted and formed an interface composed of three separate sub-layers within the interaction layer. Presence of a dendritic structure and needle-like morphology in the reaction layer that starts from base Al and continues to Mg is due to chilling nature of the insert that instantly cooled down the molten magnesium and precipitated solidification. This means that primary dendrite arms started to grow, but due to rapid cooling the secondary arms and their branches did not have the time to grow. As the columnar grains grew, temperature gradient decreased and as a result, crystal morphology changed and equiaxed grains formed (Ref 20).

By increasing the V_m/V_s ratio, interface thickness increased. For instance, reaction interface thickness of the specimen with $V_m/V_s = 5.25$ is approximately 1800 μm which is three times the interface thickness of specimen with $V_m/V_s = 3$ (i.e., 600 μm) and that is three times the thickness of the specimen with $V_m/V_s = 1.25$ (i.e., 200 μm). One may attribute this difference to the contact and solidification times of the melt and solid insert. The more the superheat or the V_m/V_s ratio, the more the melt is in contact with solid insert due to larger enthalpy. Therefore, more reaction and diffusion occurred between melt and the insert so that the resulting interface thickness increased. In another word, by decreasing the V_m/V_s and consequently decreasing the melt heat content, alloy temperature shifts from molten state to pasty zone state. This observation has also been reported by other researchers (Ref 21). Entering the pasty zone

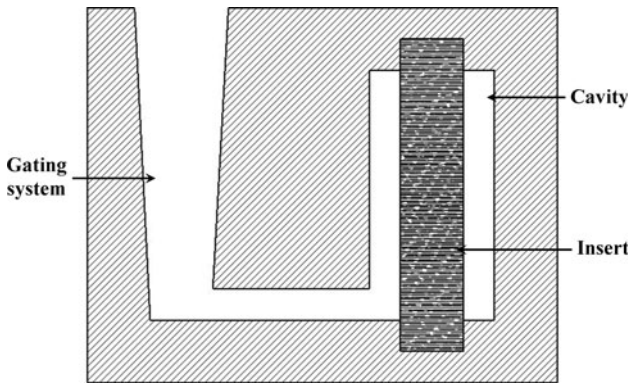

Fig. 1 Schematic sketch of the mold used in this work

Table 1 Chemical compositions (wt.%) of the commercially materials used in this study

Material	Al	Mg	Zn	Sn	Mn	Cu	Fe	Si
Aluminum	99.548	0.027	0	0.076	0.009	0.002	0.0171	0.131
Magnesium	0	99.847	0.093	0	0.017	0.012	0.002	0.029

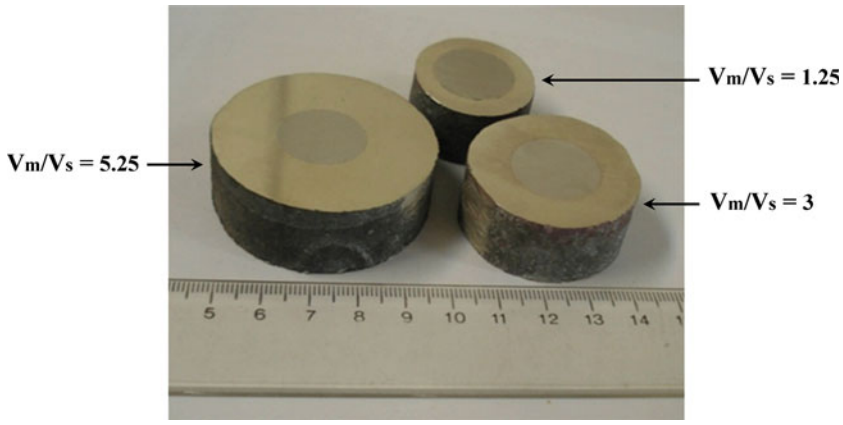

Fig. 2 The cross section of Al/Mg specimens prepared through compound casting process with different V_m/V_s

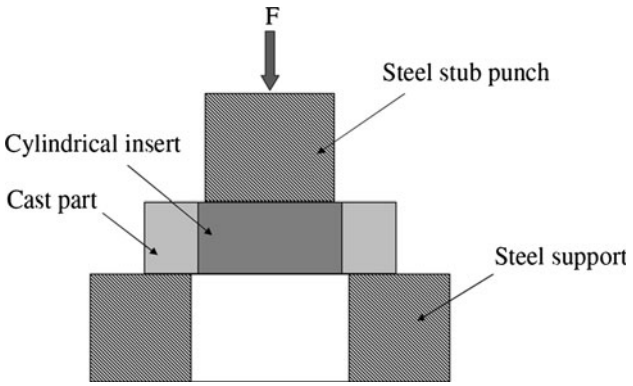

Fig. 3 Schematic sketch of the setup used for push-out tests

can reduce diffusion of the elements present in alloy and finally can cause a decrease in the interface thickness.

In addition to an increase in reaction layer thickness with higher volume ratio, some pores also were detected in the thicker interfaces. For instance, in the specimen with volume ratio of 5.25 there were more pores which are rather continuous compared to the specimen with volume ratio of 3. This could be due to formation of intermetallic compounds according to Yan et al. (Ref 22). It is evident from the Al-Mg phase diagram (Fig. 5) that Al-Mg intermetallics due to low melting points form in Mg melt/Al insert interface in the last stages of solidification. Formation of these compounds under mentioned conditions (i.e., in the last stages of solidification) is accompanied by shrinkage formatting at the reaction interface.

In order to characterize the phases formed during this process, x-ray diffraction (XRD) patterns were obtained from the specimen with the ratio of V_m/V_s equal to 3. The results are illustrated in Fig. 6. According to XRD pattern (Fig. 6), one can see that $Al_{12}Mg_{17}$, Al_3Mg_2, and Mg were formed in the interface.

For further investigating the phases formed in the reaction sub-layers, EDS point and line scans in addition to EDS were obtained from the specimen with volume ratio of 1.25.

Figures 7 and 8 demonstrate EDS maps and line scan analysis of the specimen cast with the above-mentioned volume ratio. One can see that magnesium content (green color) gradually decreases across interface from bulk magnesium to aluminum insert and it is exactly vice versa for aluminum (red).

It is noteworthy that across the interface, the curve corresponding to magnesium (green line) is almost above the curve of the aluminum (red line) except in a small region of the interface close to aluminum (layer I). This indicates that compounds with higher Mg content comprise a large portion of the microstructure.

Point analysis and EDS results performed on various zones, Fig. 7(a) and 9 shows the interface is constituted from three sub-layers. Atomic percentage of Al and Mg in each of these sub-layers was measured and the results are presented in Tables 2 and 3 for the specimens cast with 1.25 and 3 volume ratios, respectively.

Referring to the literature (Ref 16, 23-25) Al-Mg phase diagram (Fig. 5) and the results of quantitative analysis, one can conclude that in these two specimens, the microstructure near to Al insert (sub-layer I) is composed of Al_3Mg_2, while due to $L \xrightarrow{473} Al_{12}Mg_{17} + (Mg)$, the sub-layer adjacent to Mg (sub-layer III) is composed of $Al_{12}Mg_{17} + (Mg)$ eutectic structure and according to Al and Mg contents, sub-layer II composition is $Al_{12}Mg_{17}$.

Microstructure of the specimen with V_m/V_s equals to 5.25 was similar to that of other specimens and the only difference observed was in intermediate layer microstructure. Figure 10 and the results shown in Table 4 indicate a mixture of $Al_{12}Mg_{17}$ and Al in Mg solid solution eutectic structure (i.e., $Al_{12}Mg_{17}$/(Mg)) is distributed in this region in a way that by approaching sub-layer III, magnesium content increases and as a result $Al_{12}Mg_{17}$/(Mg) eutectic structure increases. Inversely by approaching reaction sub-layer I, Al content increases and as a result $Al_{12}Mg_{17}$/(Mg) eutectic phase decreases. Therefore, one may conclude that the major portion of layer II structure in this specimen is composed of $Al_{12}Mg_{17}$/(Mg) eutectic structure dispersed in $Al_{12}Mg_{17}$ intermetallic compound.

When $V_m/V_s = 5.25$, contact time between melt and solid increased and the reaction between them also increased. This resulted in reaction between melt and insert which led to formation of eutectic compound in intermediate layer of the interface. Hence, the difference in microstructure of this specimen and those referred earlier can be attributed to higher ratio of V_m/V_s.

Figure 11 shows the microstructure of interface in the specimen with V_m/V_s equals to 1.25. The microstructure of interface in specimen with V_m/V_s equals to 3 is similar to that shown in Fig. 11. Figure 12 demonstrates the microstructure of the intermediate reaction layer in specimen with $V_m/V_s = 5.25$.

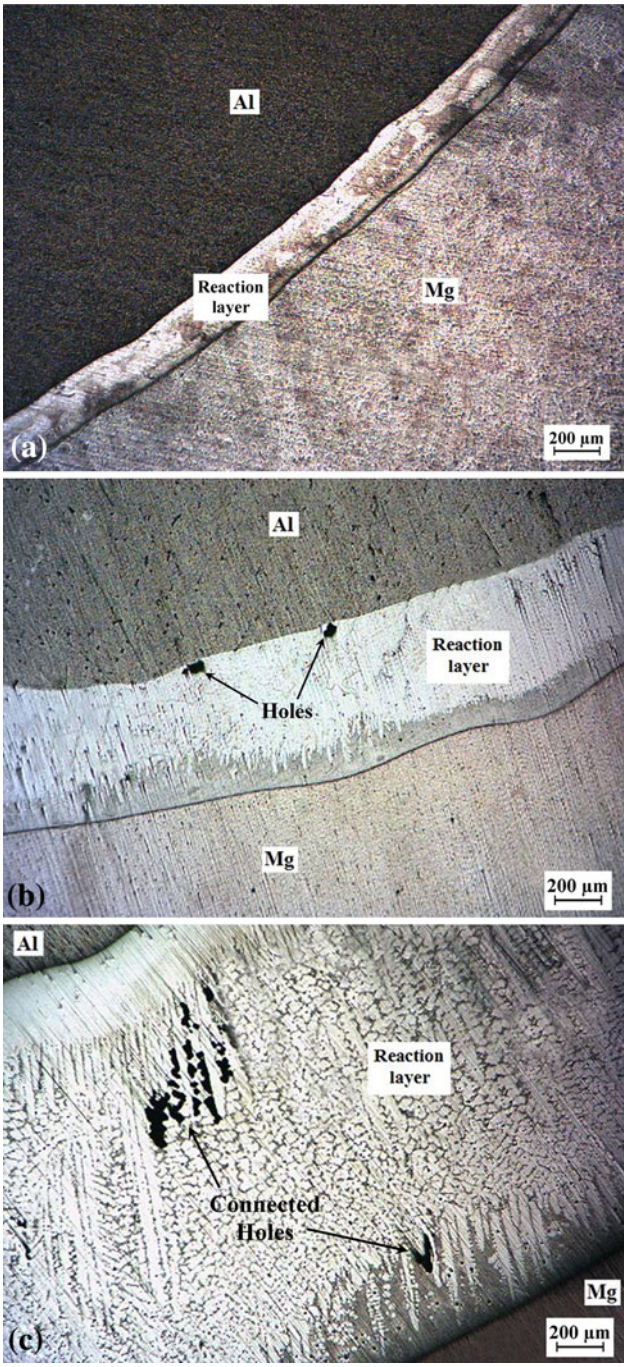

Fig. 4 OM images of the interfaces formed in specimens with various melt/solid volume ratios. (a) $V_m/V_s = 1.25$, (b) $V_m/V_s = 3$, and (c) $V_m/V_s = 5.25$

From metallurgical point of view, the presence of diffusion regions near two base alloys can be due to diffusion of Mg atoms into solid Al after the contact between molten Mg and Al insert is made. As time elapses, number of diffused atoms increases and a solid solution of Mg in Al forms. In the next step, intermetallics with lower melting points than those of two elements can be formed and finally a very thin layer of melt between Al insert and solidifying melt can appear. This thin layer of melt can be formed throughout the Al insert, since the diffusion coefficient of the elements in liquid state is much higher than that of solid state, and therefore the liquid layer can

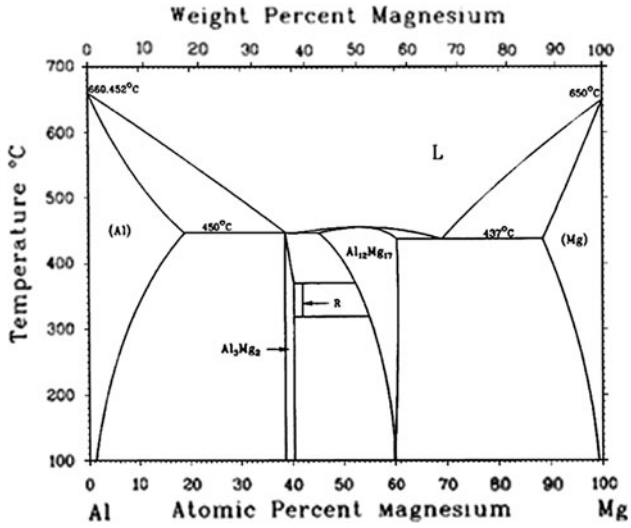

Fig. 5 Equilibrium phase diagram of Al-Mg (Ref 18)

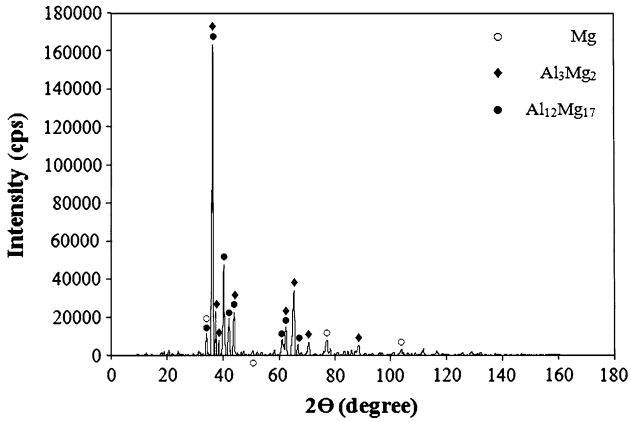

Fig. 6 XRD patterns of the interface formed in the specimen with $V_m/V_s = 3$ prepared by compound casting

facilitate the formation of Mg/Al interdiffusion zone. Thus, the liquid layer thickness could increase by the end of solidification. Finally, as liquid layer temperature decreases from experiment temperature to room temperature, solidification of the eutectic phases (i.e., $Al_{12}Mg_{17}$ and Al_3Mg_2 intermetallics) occurs (Ref 26). EDS results confirmed this results.

Two different mechanisms for formation of Al-Mg intermetallics throughout compound casting process are probable: diffusion-reaction and fusion-solidification (Ref 27, 28).

- Diffusion-reaction mechanism occurs after contact between Mg melt and Al insert is made, so that Mg and Al atoms diffuse into each other lattices and after reaching a certain concentration, diffused atoms react with host atoms and form $Al_{12}Mg_{17}$, Al_3Mg_2, and AlMg intermetallics in the interface (Ref 27).
- Fusion-solidification mechanism occurs after the contact between liquid Mg and solid Al insert is made. In this case, partial fusion of Al surface occurs and dissolves into the surrounding Mg melt. Under the mentioned circumstances, after cooling down and solidification of the melt, depending on the extent of Al dissolution in Mg melt and according to Al-Mg phase diagram (Fig. 5), $Al_{12}Mg_{17}$,

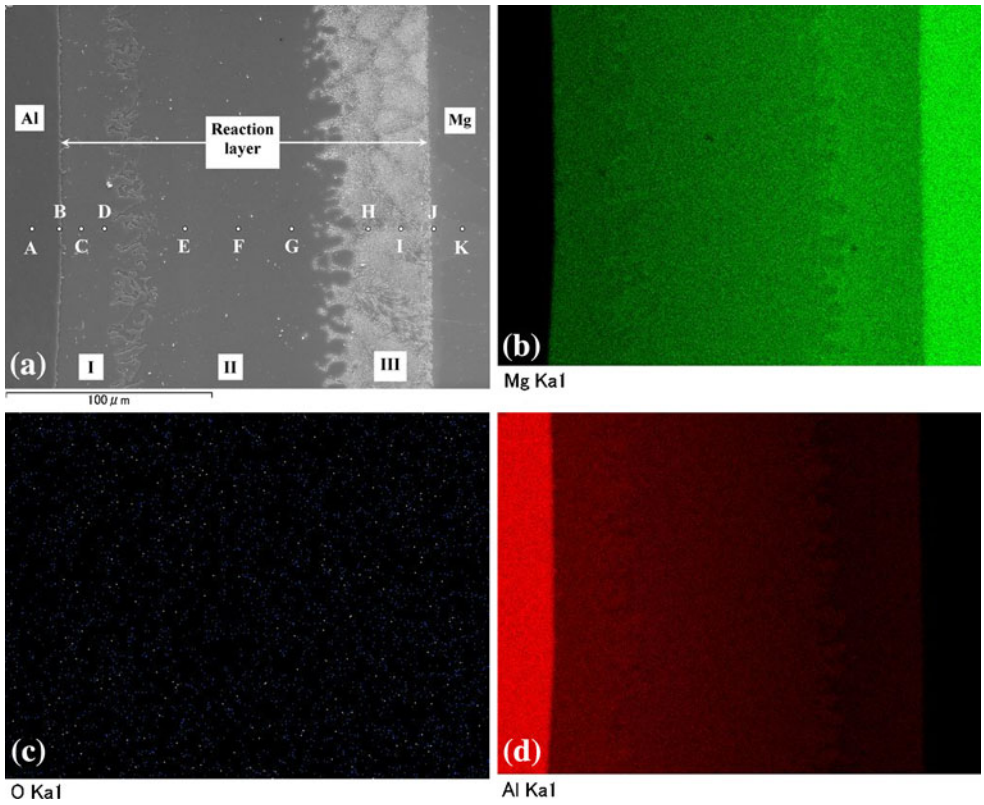

Fig. 7 EDS maps of the reaction interface in the specimen with V_m/V_s = 1.25. (a) SEM micrograph, (b) magnesium, (c) oxygen, and (d) aluminum distribution maps (Color figure online)

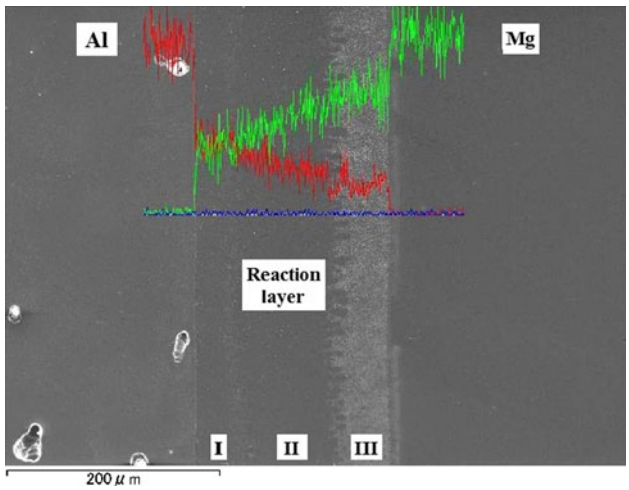

Fig. 8 Line scan analysis taken from the reaction interface of the specimen with V_m/V_s = 1.25 (Color figure online)

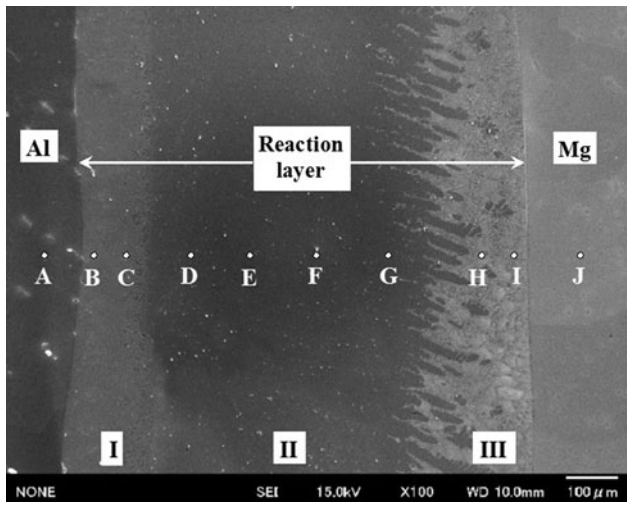

Fig. 9 Location of the points analyzed in the interface of the specimen with V_m/V_s = 3

Al_3Mg_2, and AlMg intermetallic compounds form in different regions of reaction interface (Ref 20, 28).

Figure 4 shows that in lower V_m/V_s ratio the dominant mechanism is diffusion-reaction. However, by increasing V_m/V_s ratio and contact time the probability of increasing the surface fusion of Al insert increases and therefore the dominant mechanism can be fusion-solidification. Formation of shrinkage in reaction interface of the specimens with high V_m/V_s ratio verifies that this mechanism is dominant.

Hardness tests were performed across interface of the specimens. The obtained results showed in Fig. 13 indicate that the hardness of the interface in all the three specimens is higher than those of Al and Mg base metals. This can be due to the formation of hard Al-Mg intermetallics (Ref 7, 29). Thus, one can say that an increase in hardness of reaction sub-layers can be justified by the microstructure changes explained previously.

The maximum hardness in specimens with V_m/V_s equals to 1.25, 3, and 5.25 are HV252, HV257, and HV232, respectively. The mean hardness in regions corresponding to specimens with

Table 2 Results of concentration analysis corresponding to the points indicated in Fig. 7(a)

Area number	Layer code	Element compositions (at.%)		Element compositions ratio (Al/Mg)	Inference component
		Al	Mg		
A	Al	100	0	…	Al
B		84.71	15.29	5.54	(Al)
C	I	59.98	40.02	1.50	Al_3Mg_2
D		59.78	40.22	1.49	Al_3Mg_2
E	II	48.00	52.00	0.92	$Al_{12}Mg_{17}$
F		46.55	53.45	0.87	$Al_{12}Mg_{17}$
G		45.90	54.10	0.85	$Al_{12}Mg_{17}$
H	III	29.19	70.81	0.41	$Al_{12}Mg_{17}$/(Mg)
I		28.98	71.02	0.41	$Al_{12}Mg_{17}$/(Mg)
J	Mg	12.54	87.46	0.14	(Mg)
K		0	100	…	Mg

(Mg), Magnesium solid solution

Table 3 Results of concentration analysis corresponding to the points shown in Fig. 9

Area number	Layer code	Element compositions (at.%)		Element compositions ratio (Al/Mg)	Inference component
		Al	Mg		
A	Al	100	0	…	Al
B	I	60.14	39.86	1.51	Al_3Mg_2
C		59.32	40.68	1.45	Al_3Mg_2
D	II	49.30	50.70	0.97	$Al_{12}Mg_{17}$
E		45.88	54.12	0.85	$Al_{12}Mg_{17}$
F		48.76	51.24	0.95	$Al_{12}Mg_{17}$
G		42.40	57.60	0.74	$Al_{12}Mg_{17}$
H	III	29.58	70.42	0.42	$Al_{12}Mg_{17}$/(Mg)
I		25.81	74.19	0.35	$Al_{12}Mg_{17}$/(Mg)
J	Mg	0	100	…	Mg

(Mg), Magnesium solid solution

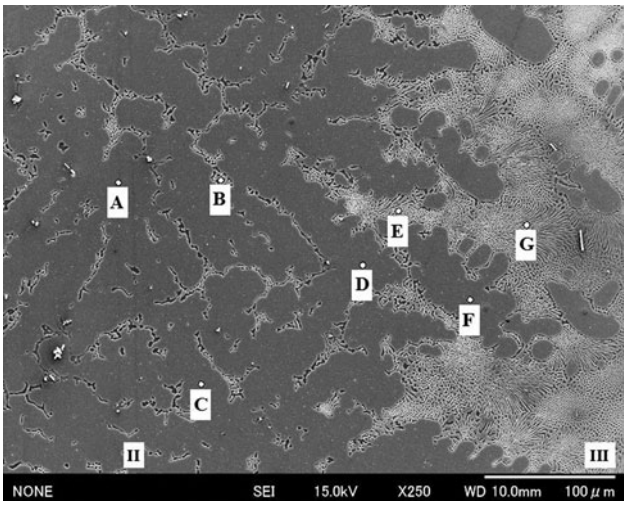

Fig. 10 Location of the points analyzed in layer II of the specimen with $V_m/V_s = 5.25$

Table 4 Results of the concentration analysis corresponding to the points indicated in Fig. 10

Area number	Element compositions (at.%)		Element compositions ratio (Al/Mg)	Inference component
	Al	Mg		
A	38.64	61.36	0.63	$Al_{12}Mg_{17}$
B	31.19	68.81	0.45	$Al_{12}Mg_{17}$/(Mg)
C	37.18	62.82	0.59	$Al_{12}Mg_{17}$
D	38.21	61.79	0.62	$Al_{12}Mg_{17}$
E	31.57	68.43	0.46	$Al_{12}Mg_{17}$/(Mg)
F	36.92	63.08	0.58	$Al_{12}Mg_{17}$
G	21.69	78.31	0.28	$Al_{12}Mg_{17}$/(Mg)

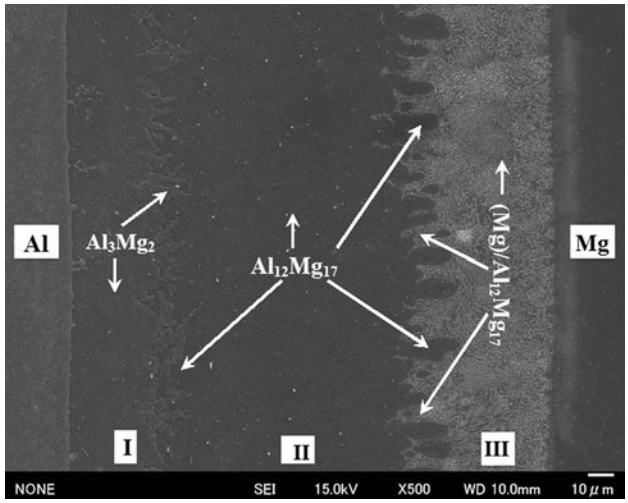

Fig. 11 Microstructure of the interface formed in specimen with $V_m/V_s = 1.25$

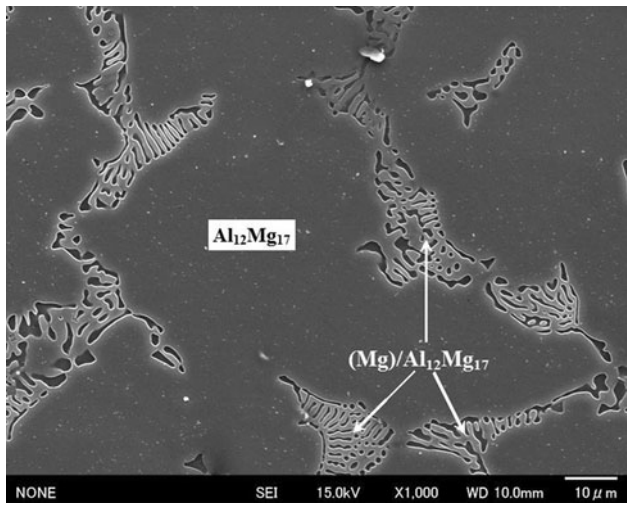

Fig. 12 SEM micrograph from layer II in reaction interface of the specimen with $V_m/V_s = 5.25$

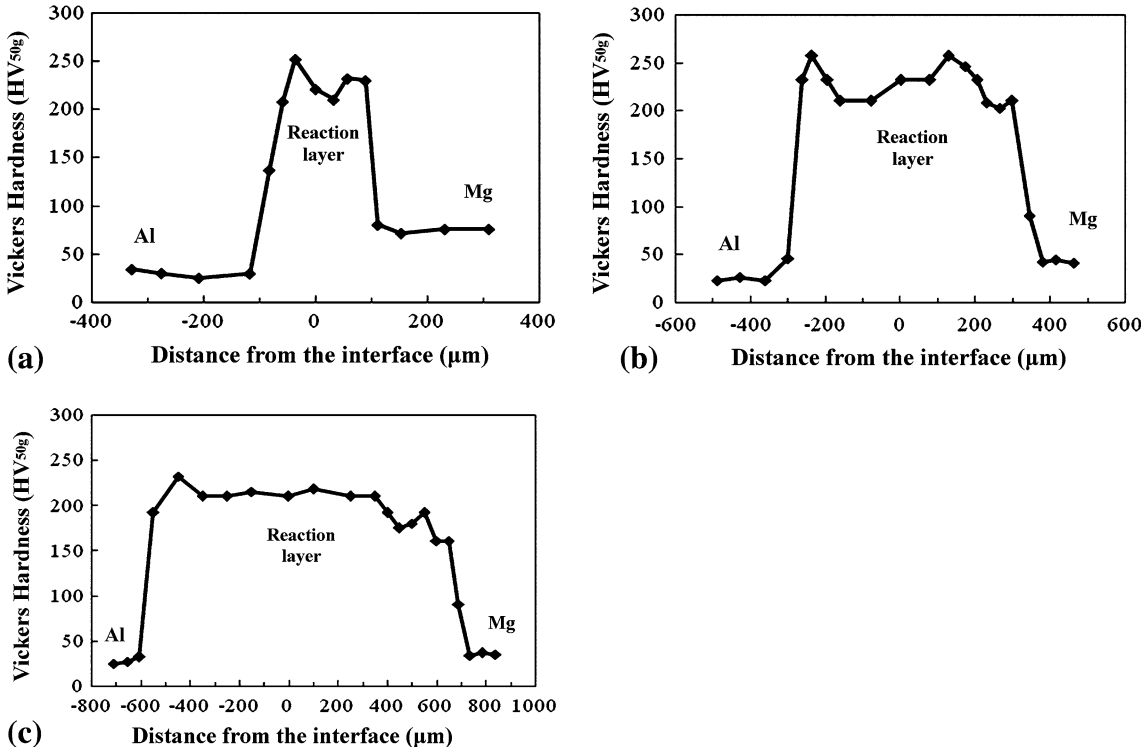

Fig. 13 Microhardness versus distance from interface center in compound cast specimens with V_m/V_s. (a) 1.25, (b) 3, and (c) 5.25

Table 5 Shear strength of the Al/Mg couples prepared at different V_m/V_s

V_m/V_s	Thickness of the interface, μm	Test number	Maximum sher load, kN	Shear strength, MPa	Average shear strength, MPa
1.25	200	1	18.3	29.1	27.1
		2	15.9	25.3	
		3	16.9	26.9	
3	600	1	10.2	16.2	15.1
		2	10	15.9	
		3	8.3	13.2	
5.25	1800	1	6.8	10.8	8.3
		2	4.2	6.7	
		3	4.6	7.3	

V_m/V_s ratio equals to 1.25, 3, and 5.25 are HV212.86, HV245.61, and HV197.87, respectively. Therefore, it is evident that hardness of the specimen with V_m/V_s equals to 3 is higher than those of other two which indicates that this volume ratio resulted to formation of a type of interface having the highest hardness. On the other hand, hardness near Mg bulk metal decreases a little which is probably due to presence of $Al_{12}Mg_{17}$ + (Mg) eutectic structure in the layer on the Mg side. The presence of magnesium solid solution in sub-layer III which has a lower hardness compared to Al-Mg intermetallics causes a decrease in hardness of this reaction layer compared to those of the other two layers which are composed of hard Al-Mg intermetallics. The results of push-out shear strength tests for the Al/Mg couples prepared at different V_m/V_s ratios are listed in Table 5.

The average shear strengths of the interface decrease from 27.1 to 15.1 and 8.3 MPa for the Al/Mg couples prepared at 1.5, 3, and 5.25 V_m/V_s respectively. Decrease in shear strength of the interface seems to be due to increasing the interface thickness and consequently increasing the amount of brittle and high hardness Al_3Mg_2 and $Al_{12}Mg_{17}$ intermetallic compounds. In addition, the presence of porosities at the interface of Al/Mg couples prepared at higher V_m/V_s (3 and 5.25) has significant effect on decreasing the shear strength of these samples (Fig. 4b, c).

4. Conclusions

1. Bonding of magnesium and aluminum metals can be done via compound casting.
2. Thickness of the reaction layer formed between Mg and Al depends on the melt-to-solid insert volume ratio and by increasing this ratio not only the thickness of the reaction interface increases but also larger and continuous shrinkage pores can be formed in the reaction interface microstructure.

3. Formation of the interface through Mg and Al dissimilar metals bonding via compound casting is diffusion controlled in low volume ratios while at high volume ratios the dominant mechanism is fusion-solidification.
4. The interface formed through bonding of Mg and Al via compound casting in composed of three sub-layers: the sub-layers adjacent to Al and Mg base metals comprise Al_3Mg_2 intermetallic and $Al_{12}Mg_{17}$/(Mg) eutectic, respectively. While the middle sub-layer microstructure in the specimens with low V_m/V_s is mainly $Al_{12}Mg_{17}$ and in specimens with high V_m/V_s is $Al_{12}Mg_{17}$/(Mg) eutectic structure.
5. Due to formation of hard and brittle intermetallics of Al-Mg, hardness of the reaction layer formed between Al and Mg metals cast via compound casting is higher than both Al and Mg base metals.
6. Shear strengths of the interface decrease from 27.1 to 15.1 MPa and finally to 8.3 MPa for the Al/Mg couples having 1.5, 3, and 5.25 V_m/V_s ratios, respectively, due to increase of the interface thickness.

Acknowledgments

Herewith the authors would like to acknowledge the assistance of Professor T. Homma and his colleagues for the contribution.

References

1. J.R. Davis, *Aluminum and Aluminum Alloys, ASM Specialty Handbook*, ASM International, Materials Park, OH, 1993
2. M.M. Avedesian and H. Baker, *Magnesium and Magnesium Alloys, ASM Specialty Handbook*, ASM International, Materials Park, OH, 1998
3. B.K. Amoid, T. Heijkoop, P.G. Lloyd, G. Rubenis, and I.R. Sare, Wear of Cast-Bonded Components in a Coal Pulveriser Mill, *Wear*, 1997, **203–204**, p 663–670
4. K.J.M. Papis, J.F. Loeffler, and P.J. Uggowitzer, Light Metal Compound Casting, *Sci. China E*, 2009, **52**, p 46–51
5. K.J.M. Papis, B. Hallstedt, J.F. Loeffler, and P.J. Uggowitzer, Interface Formation in Aluminium-Aluminium Compound Casting, *Acta Mater.*, 2008, **56**, p 3036–3043
6. N. Horikawa, T. Ito, T. Noguchi, and T. Nakamura, Size Effect in Cast-In Insertion Process, *Int. J. Cast Met. Res.*, 2003, **16**, p 365–369
7. T. Noguchi, N. Horikawa, H. Nagate, T. Nakamura, and K. Sato, Application of Flow and Solidification Simulation in Cast-In Insertion Processing, *Int. J. Cast Met. Res.*, 2005, **18**, p 214–220
8. T. Heijkoop and I.R. Sare, Cast-Bonding: A New Process for Manufacturing Composite Wear Products, *Cast Met.*, 1989, **2**, p 160–168
9. T. Noguchi, S. Kamota, T. Sato, and M. Sakai, Use of Thermal Spraying to Enhance Bonding of Steel Cast-In Inserts in Cast Iron, *AFS Trans.*, 1993, **89**, p 231–239
10. A. Avci, N. Ilkaya, M. Simsir, and A. Akdemir, Mechanical and Microstructural Properties of Low-Carbon Steel-Plate-Reinforced Gray Cast Iron, *J. Mater. Process. Technol.*, 2009, **209**, p 1410–1416
11. J. Pan, M. Yoshida, G. Sasaki, H. Fukunaga, H. Fujimura, and M. Matsuura, Ultrasonic Insert Casting of Aluminum Alloy, *Scripta Mater.*, 2000, **43**, p 155–159
12. K.H. Choe, K.S. Park, B.H. Kang, G.S. Cho, K.Y. Kim, K.W. Lee, M.H. Kim, A. Ikenaga, and S. Koroyasu, Study of the Interface Between Steel Insert and Aluminum Casting in EPC, *J. Mater. Sci. Technol.*, 2008, **24**, p 60–64
13. M. Divandari and A.R. Vahid Golpayegani, Study of Al/Cu Rich Phases Formed in A356 Alloy by Inserting Cu Wire in Pattern in LFC Process, *Mater. Des.*, 2009, **30**, p 3279–3285
14. M. Scanlan, D.J. Browne, and A. Bates, New Casting Route to Novel Functionally Gradient Light Alloys, *Mater. Sci. Eng., A*, 2005, **413–414**, p 66–71
15. K.J.M. Papis, J.F. Loffler, and P.J. Uggowitzer, Interface Formation Between Liquid and SOLID MG ALLOYS—An Approach to Continuously Metallurgic Joining of Magnesium Parts, *Mater. Sci. Eng., A*, 2010, **527**, p 2274–2279
16. E. Hajjari, M. Divandari, S.H. Razavi, S.M. Emami, T. Homma, and S. Kamado, Dissimilar Joining of Al/Mg Light Metals by Compound Casting Process, *J. Mater. Sci.*, 2011, **46**, p 6491–6499
17. T. Noguchi, N. Horikawa, H. Nagate, T. Nakamura, and K. Sato, Application of Flow and Solidification Simulation in Cast-In Insertion Processing, *Int. J. Cast Met. Res.*, 2005, **18**, p 214–220
18. M. Sacerdote-Peronnet, E. Guiot, F. Bosselet, O. Dezellus, D. Roubyb, and J.C. Viala, Local Reinforcement of Magnesium Base Castings with Mild Steel Inserts, *Mater. Sci. Eng., A*, 2007, **445–446**, p 296–301
19. O. Dezellus, L. Milani, F. Bosselet, M. Sacerdote-Peronnet, D. Rouby, and J.C. Viala, Mechanical Testing of Titanium/Aluminium-Silicon Interfaces by Push-Out, *J. Mater. Sci.*, 2008, **43**, p 1749–1756
20. Y. Gao, C. Wang, Q. Lin, H. Liu, and M. Yao, Broad-Beam Laser Cladding of Al-Si Alloy Coating on AZ91HP Magnesium Alloy, *Surf. Coat. Technol.*, 2006, **201**, p 2701–2706
21. Alloy Phase Diagrams, ASM Hand Book, Vol. 3, 9th ed., Materials Park, OH, 1995
22. J. Yan, Z. Xu, Z. Li, L. Li, and S. Yang, Microstructure Characteristics and Performance of Dissimilar Welds Between Magnesium Alloy and Aluminum Formed by Friction Stirring, *Scripta Mater.*, 2005, **53**, p 585–589
23. D. Singh, C. Suryanarayana, L. Mertus, and R.-H. Chen, Extended Homogeneity Range of Intermetallic Phases in Mechanically Alloyed Mg-Al Alloys, *Intermetallics*, 2003, **11**, p 373–376
24. J.R. Cahoon, Discussion of Microstructure and Phase Constituents in the Interface Zone of Mg/Al Diffusion Bonding, *Metall. Mater. Trans. B*, 2007, **38B**, p 109–112
25. L. Peng, L. Yajiang, G. Haoran, W. Juan, M.A. Haijun, and G. Guolin, Microstructure and Phase Constituents in the Interface Zone of Mg/Al Diffusion Bonding, *Metall. Mater. Trans. B*, 2006, **37**, p 649–654
26. F. Liu, X. Li, W. Liang, X. Zhao, and Y. Zhang, Effect of Temperature on Microstructures and Properties of Aluminized Coating on Pure Magnesium, *J. Alloys Compd.*, 2009, **478**, p 579–585
27. V.I. Dybkov, *Reaction Diffusion and Solid State Chemical Kinetics*, 1st ed., IPMS Publications, Kyiv, 2002
28. P.G. Huggett, R. Wuhrer, B. Ben-Nissan, and K. Moran, A Novel Metallurgical Bonding Process and Microstructural Analysis of Ferrous Alloy Composites, *Proceedings of the 3rd International Conference on Advanced Materials Processing*, Institute of Materials Engineering Australasia Ltd, 2004, p 83–88
29. Y.S. Sato, S. Hwan, C. Park, M. Michiuchi, and H. Kokawa, Constitutional Liquation During Dissimilar Friction Stir Welding of Al and Mg Alloys, *Scripta Mater.*, 2004, **50**, p 1233–1236